

## Histological and Immunohistochemical Study on the Possible Therapeutic Effect of Bone Marrow-Derived Mesenchymal Stem Cells on L-arginine-Induced Acute Pancreatitis in Adult Male Albino Rat

Leila F. Ammar, Mona T. Sadek, Reda H. Elbakary and Amany M. Mousa

Department of Histology and Cell Biology, Faculty of Medicine, Tanta University, Egypt

### ABSTRACT

**Introduction :** Acute Pancreatitis (AP) is a severe inflammatory disease that has no particular therapy. Due to their capacity for self renewal and multipotency, bone marrow-derived mesenchymal stem cells (BM-MSCs) provide a viable therapeutic option.

**Aim of the Work:** The purpose of this study was to determine the possible therapeutic effect of bone marrow-derived mesenchymal stem cells (BM-MSCs) on acute pancreatitis induced by L-arginine in adult male albino rats.

**Materials and Methods:** Three main groups of 45 adult male albino rats were established.; group I served as a control and included; subgroup IA (served as the source of BM-MSCs), subgroup IB (animals received 2.5 ml of saline once intraperitoneally) and subgroup IC (animals received 2.5 ml of saline once intraperitoneally followed one hour later by intravenous injection of 1 ml of ordinary media via the tail vein). Group II: animals were injected by 2.5 ml of 20% L-arginine once intraperitoneally for induction of AP while group III: animals were injected with 1 ml ( $1 \times 10^6$ ) of BM-MSCs suspended in ordinary media through the tail vein one hour after induction of AP. Blood samples were collected to measure serum amylase and lipase levels at 24 hours and 72 hours. Then, rats were sacrificed at 72 hours and pancreatic specimens were processed for histological and immunohistochemical studies by the light microscope.

**Results:** In comparison to the untreated group II, group III treated with BM-MSCs exhibited substantial improvement in pancreatic histological structure and pancreatic enzyme levels.

**Conclusion:** BM-MSCs exerted a significant ameliorative therapeutic effect on exocrine pancreatic tissue after AP induction.

**Received:** 23 September 2021, **Accepted:** 05 November 2021

**Key Words:** Acute pancreatitis, BM-MSCs, l-arginine, prussian blue stain.

**Corresponding Author:** Leila F. Ammar, MSc, Department of Histology and Cell Biology, Faculty of Medicine, Tanta University, Egypt, **Tel.:** +2 012 7228 9770, **E-mail:** leila.ammar@med.tanta.edu.eg

**ISSN:** 1110-0559, Vol. 46, No.1

### INTRODUCTION

Acute pancreatitis (AP) is one of the most common acute pancreatic disorders that is considered an extremely life-threatening inflammatory condition with rising incidences<sup>[1]</sup>. Acute pancreatitis has a significant death rate, which may be explained by a systemic inflammatory response and various organ dysfunction syndromes. Despite the considerable progress that has been made over the past decades in treatment of diseases, still there is no available specific therapy to limit the progression of AP. The current treatment is only supportive and is restricted to fluid therapy, nutritional support, treatment of infection and analgesics<sup>[2,3]</sup>.

The L-arginine-induced acute pancreatitis model is a commonly used laboratory model that closely resembles the human phenotype of AP in many aspects. Although the mechanisms behind L-arginine-induced AP are complex, activation of digesting enzymes inside acinar cells has been acknowledged as the initiating event, while oxygen

and nitrogen free radicals play a significant role in AP development<sup>[4,5]</sup>.

Stem cells are a tiny population of undifferentiated cells that are found throughout the living body. These cells are defined by their capacity to generate "progenitor" cells capable of maturation into mature and differentiated cells. Additionally, stem cells are capable of asymmetric division and self-renewal. All these qualities give the stem cells a great interest for use in therapeutic applications to replace damaged tissues and cells in various medical conditions<sup>[6,7]</sup>.

Mesenchymal stem cells (MSCs) are multipotent cells with high proliferation, differentiation and self-healing capacities. They can be isolated from many tissues such as adipose tissue, umbilical cord, amniotic fluid and dental pulp but the bone marrow is considered the main source. Previous studies showed that MSCs can migrate to the site of tissue damage and have potential therapeutic value in many pancreatic disorders<sup>[8,9]</sup>.

It is useful to monitor and observe the cell dispersion of transplanted cells in the assessment of cellular therapy applications. Iron labeling is one of the direct cell tracers which can be used in both *in vivo* and *in vitro* studies. It doesn't affect the cell viability and self-renewal capacity of MSCs<sup>[10,11]</sup>.

This study was carried out to examine the prospective therapeutic effect of mesenchymal cells generated from the bone marrow on L-arginine-induced acute pancreatitis in adult male albino rat using biochemical, histological and immunohistochemical methods.

## MATERIALS AND METHODS

### Experimental design

Forty five adult male albino rats weighing 180–200 gram each were used in this work. For two weeks before to the commencement of the experiment, the animals were kept under adequate illumination and ventilation in plastic cages with mesh wire and free access to laboratory feed and water to acclimate, as recommended by The National Research Council of the National Academies (2011)<sup>[12]</sup>. The Research Ethical Committee of the Faculty of Medicine of Tanta University authorised all experimental methods. The rats were split into three main groups (15 rats each);

**Group I (Control group):** that were further randomly subdivided into three equal subgroups (five rats each):

- Subgroup IA: animals were kept without treatment to serve as the source of the stem cells. The bone marrow was collected from both tibias and femurs of each rat.
- Subgroup IB: animals received 2.5 ml of saline once intraperitoneally.
- Subgroup IC: animals received 2.5 ml of saline once intraperitoneally followed one hour later by intravenous injection of 1 ml of ordinary media once via the tail vein.

Control subgroup rats were sacrificed at the same time points as the experimental groups. Blood samples from the control group were taken to determine the normal serum amylase and lipase levels.

**Group II (Acute pancreatitis group):** animals were given 2.5 ml of 20% L-arginine (at a dose of 250 mg/100 gm body weight) once intraperitoneally for induction of acute pancreatitis. L-arginine was obtained in the form of a powder from Sigma Chemical Company, Cairo, Egypt. L-arginine solution (20% concentration) was prepared by dissolving 2 grams of L-arginine hydrochloride in 8 ml of 0.9% saline and the volume was made up to 10 ml with saline<sup>[13]</sup>.

**Group III (BM-MSCs treated group):** animals were given L-arginine in the same way as in group II to induce acute pancreatitis. One hour after the induction, each rat was injected with 1 ml ( $1 \times 10^6$ ) of BM-MSCs suspension in ordinary media through the tail vein<sup>[14,15]</sup>.

Twenty four hours after the induction of acute pancreatitis, five rats from groups II and five rats from group III were sacrificed to obtain blood samples directly from the heart to insure the induction of AP by measuring serum levels of amylase and lipase. The remaining rats in groups II and III were sacrificed 72 hours after AP induction. Blood samples were collected for biochemical analysis and pancreatic specimens were obtained from the head of pancreas and processed for histological and immunohistochemical studies by light microscope. All the animals were anaesthetized before sacrifice by an intraperitoneal injection of 1% sodium phenobarbital at a dose of 50 mg/kg body weight<sup>[16]</sup>.

### Isolation of mesenchymal stem cells

BM-MSCs were isolated, cultured, prepared, and labelled at Tanta University's Faculty of Medicine's Histology and Cell Bioplogy department.

MSCs were isolated and primarily cultured from the bone marrow of rats' long bones using Caplan's technique<sup>[17]</sup>. The bone marrow was washed by phosphate buffered saline (PBS). Bone marrow cells were placed in a T 25 flask and supplemented with full medium (89 ml DMEM, 10 ml FBS, and 1 ml antibiotic/antimycotic mixture) to a final volume of 7 ml. The culture flasks were labelled with the cells' names, passage numbers, and dates, and then maintained at 37°C in a 5% CO<sub>2</sub> incubator. Culture and expansion of MSCs was done according to McFarlin *et al.* (2006) and Nardi and Meirelles (2008)<sup>[18,19]</sup>. The nonadherent cells were removed three days after the main culture and the media was replaced with new complete medium. Within 8–10 days, the flasks reached 70%–80% confluence and were filled with a dense homogeneous population of spindle-shaped cells developing in spiral whorls. To get passage 1 cells (P1), trypsinization and sub-culturing were used to avoid MSC clumping, which might limit their development rate.

### Tracking of iron-labeled BM-MSCs using Prussian blue stain

Iron sucrose (sacrofer) from Amoun Pharmaceutical Company (El Obour City, Cairo, Egypt) was used to label cultured cells. Iron was added to the cell medium at a concentration of 20 µl/ml two hours before MSC collection<sup>[20]</sup>. The labeled cells were detected in paraffin sections using Prussian blue (Pb) stain<sup>[21]</sup>. The slides were counter stained with fast red, so the nuclei appeared red and the cytoplasm appeared pink while the iron labeled cells appeared blue. A section of spleen was used as a positive control and was provided by Newcomer Supply.

### Histological and immunohistochemical studies of the pancreas

Pancreatic specimens were promptly fixed in 10% formalin for 24 hours before being processed and embedded in paraffin wax according to standard procedure.

### **Five micrometres-thick sections<sup>[22]</sup> were obtained for**

#### **A- Histological study**

1. Hematoxylin and eosin stains<sup>[23]</sup>.
2. Masson's trichrome stain<sup>[24]</sup>.

#### **B- Immunohistochemical study**

1. Cleaved caspase-3 immunoreaction.
2. Proliferating cell nuclear antigen (PCNA) immunoreaction.

Tissue sections were de-waxed and rehydrated by gradual descending grades of alcohol. Sections were washed twice in phosphate buffered saline (PBS). At room temperature, the slides were treated for 10 minutes in hydrogen peroxide (3%) to inactivate endogenous peroxidase and minimise nonspecific background staining. Sections were washed in phosphate buffered saline (PBS). Antigen retrieval was accomplished by immersing the slides in 0.1 mol/l citrate buffer solution (pH=6.0) and heating for 10-20 minutes in a microwave oven. Sections were allowed to cool at room temperature for 20 minutes. Slides were flushed twice with phosphate buffered saline (PBS). In some sections, rabbit polyclonal antibody to caspase-3 (Caspase-3 (Cleaved), CP 229 A, Biocare Medical) was applied all over the night at 4°C in a diluted form 1:100. In other sections, mouse monoclonal antibody to PCNA (PCNA, AM252-5M, Biogenex) was applied all over the night at 4°C in a diluted form 1:50. Slides were washed in PBS. Biotinylated goat antirabbit antibody immunoglobulin G was applied for 15 minutes. Slides were flushed with PBS. The slides were then treated with a chromogenic substrate (diaminobenzidine; DAB) until the desired reaction occurred. Following that, Mayer's hematoxylin was used to counterstain the sections. Negative control sections were produced in the same manner as positive control sections, except that the main antibody phase was omitted<sup>[25,26]</sup>. A colon cancer section served as a positive control for caspase-3, and a breast cancer section served as a positive control for PCNA. Caspase-3 immunoreaction gives cytoplasmic and nuclear brownish reaction in positive cells, while PCNA immunoreaction gives nuclear brownish reaction in positive cells.

#### **Morphometric study**

Ten different non-overlapping randomly selected fields from each slide were quantified for:

- a. The mean area percentage of collagen fibers in Masson's trichrome stained sections (at x400 magnification).
- b. The mean color density of caspase-3 immunoreaction (at x400 magnification).
- c. The mean PCNA-Labeling Index (PCNA-LI) (at x400 magnification).

PCNA-Labeling Index (PCNA-LI) was determined by dividing the number of PCNA-positive cells by the total number of cells evaluated X 100<sup>[27]</sup>.

### **Statistical Analysis**

The biochemical and morphometric measurements were expressed as means  $\pm$  standard deviation (SD) and were analysed using Graph Pad In Stat Software then compared by one way analysis of variance (ANOVA) test followed by Tukey's test to compare different groups with control group. The difference was considered statistically significant if probability value (*P value*) <0.05, highly significant if *P value* <0.001 and non-significant if *P value* >0.05<sup>[28]</sup>.

## **RESULTS**

### **General Observation**

In the present work, all rats survived along the periods of experiment and no mortality was recorded. Also, the biochemical, histological and immunohistochemical results of all subgroups of control group were similar.

#### **I- In vitro studies**

1- Morphological identification of unstained bone marrow-mesenchymal stem cells (BM-MSCs) culture using phase contrast inverted microscope:

On the 1st day of the primary culture of BM cells, the cultured cells appeared rounded in shape, crowded and floating (Figure 1). On the 9th day, fibroblast like cells having long processes with central vesicular nuclei and multiple nucleoli started to appear. They were adherent to the floor of the flask. The cells became close to each other and reached about 70%-80% confluency (Figure 2). The cells were then harvested and injected in the required count in one ml media.

2- Morphological identification of BM-MSCs culture stained by Giemsa stain using phase contrast inverted microscope:

The adherent cultured cells had a star-shaped appearance with many interdigitating processes, granular cytoplasm, and blue vesicular nuclei with prominent nucleoli. (Figure 3).

#### **II- Tracking of iron-labeled BM-MSCs using Prussian blue stain**

Detection of iron labeled BM-MSCs in pancreatic tissue was done using Prussian blue stain. Prussian blue stained pancreatic sections from group I (control group) revealed diffuse red pancreatic tissue without any blue reactivity for the Prussian blue (Figure 4). Prussian blue stained pancreatic sections from group II (acute pancreatitis group) revealed diffuse red pancreatic tissue without any blue reactivity for the Prussian blue (Figure 5). Prussian blue stained pancreatic sections from group III (BM-MSCs treated group) revealed sporadic reaction of Prussian blue stain that BM-MSCs appeared as detectable blue dots within the red pancreatic tissue (Figure 6).

#### **III- Histological and immunohistochemical studies of the pancreas**

Light microscopic examination of sections obtained

from group I revealed normal histological features of pancreas. The exocrine pancreas was composed of densely packed, almost spherical secretory acini arranged in lobules and separated by small interlobular spaces containing blood vessels and ducts. The acinar cells showed basal cytoplasmic basophilia, apical acidophilic secretory granules and basal spherical pale nuclei. The lumen of the acini contained small low cuboidal cells with pale cytoplasm called centroacinar cells (Figures 7,8). Minimal amount of fine collagen fibers appeared around the blood vessels, interlobular ducts and in between the pancreatic lobules (Figure 9). Caspase-3 immunostained sections revealed a weak positive cytoplasmic brownish reaction in few acinar cells (Figure 10), while PCNA immunostained sections revealed few acinar cells with positive nuclear brownish reaction (Figure 11).

Light microscopic examination of group II indicated loss of the normal pancreas architecture with evident histological changes in its exocrine portion in the form of widely separated lobules and disorganized widely separated acini. Some lobules revealed disorganization and partial destruction of some acini. Many acinar cells appeared separated from each other. Some acinar cells showed large cytoplasmic vacuoles compressing the nuclei leading to peripheral flattened nuclei. In addition, some acinar cells appeared with dark basophilic cytoplasm (Figure 12). Some acinar cells were lysed with appearance of homogenous acidophilic material in between the acini. Moreover, some acinar cells showed dark nuclei with perinuclear halos (Figure 13). Dilated and congested blood vessels with vacuolation of the tunica media layer of their walls were detected (Figure 14). Moreover, some interlobular ducts were dilated with irregularity of their walls while other ducts were lined with flattened epithelial cells (Figure 15). Additionally, mononuclear inflammatory cells were detected around the dilated blood vessels and interlobular ducts (Figures 14,15). Dense collagen fibers developed inbetween the acini, surrounding dilated blood vessels, and dilated ducts (Figures 16,17). Caspase-3 immunostained sections revealed an intense positive cytoplasmic brownish reaction in many acinar cells (Figure 18), while PCNA immunostained sections revealed many acinar cells with positive nuclear brownish reaction (Figure 19).

Light microscopic examination of group III revealed apparent preservation of the normal histological pancreatic architecture. The majority of pancreatic acini seemed to be more or less normal with narrow interlobular spaces. The majority of acinar cells had basal basophilia, apical acidophilia with many zymogen granules, and basal nuclei with prominent nucleoli (Figure 20). However, few acinar cells showed dark basophilic cytoplasm (Figure 21). As regards the interlobular ducts, most ducts appeared more or less normal and are lined by a single layer of cuboidal cells (Figure 21). Little amount of collagen fibres were detected inbetween the acini, surrounding the blood vessels and the ducts (Figure 22). Caspase-3 immunostained sections

revealed a weak positive cytoplasmic brownish reaction in few acinar cells (Figure 23), while PCNA immunostained sections revealed few acinar cells with positive nuclear brownish reaction (Figure 24).

### Statistical results

1- Laboratory investigations (Serum amylase and lipase levels) (Tables 1,2 - Bar charts 1,2):

Statistical analysis of the collected data showed that group II (acute pancreatitis group) had a highly significant increase ( $P$  value  $<0.001$ ) in serum amylase and lipase levels at 24 and 72 hours when compared to group I (control group). On the other hand, group III (BM-MSCs treated group) demonstrated a significant decrease in the mean serum amylase and lipase levels ( $P$  value  $<0.05$ ) when compared to group II and a significant increase in the mean serum amylase and lipase levels when compared to group I.

2- Area percentage of collagen fibers:

The mean value of area percentage of collagen fibers in Masson's trichrome stained sections (Table 3 - Bar chart 3):

Statistical analysis of the data collected by image J analysis program revealed a significant increase ( $P$  value  $<0.05$ ) of the mean area percentage of collagen fibers in group II (acute pancreatitis group) when compared to group I (control group). However, in group III (BM-MSCs treated group), there was a significant decrease in the mean area percentage of collagen fibers when compared to group II and a non significant increase ( $P>0.05$ ) when compared to group I.

3- Color density of caspase-3 immunoreactivity:

The mean value of color density of caspase-3 immunoreactivity (Table 4 - Bar chart 4):

Statistical analysis of the data collected by image J analysis program revealed a significant increase ( $P$  value  $<0.05$ ) in the mean colour density of caspase-3 immunoreactivity in group II (acute pancreatitis group) as compared to group I (control group). Group III (BM-MSCs treated group) demonstrated a significant decrease in the mean colour density of caspase-3 immunoreactivity when compared to group II and a non significant increase ( $P>0.05$ ) when compared to group I.

4- PCNA-Labeling Index immunoreactivity:

The mean value of PCNA-Labeling Index immunoreactivity (Table 5 - Bar chart 5):

Statistical analysis of the data collected by image J analysis program showed a significant increase ( $P$  value  $<0.05$ ) in the mean value of PCNA-Labeling Index immunoreactivity in group II as compared to group I (control group). Group III (BM-MSCs treated group) showed a significant decrease in the mean value of PCNA-Labeling Index immunoreactivity as compared to group II and a non significant increase ( $P>0.05$ ) as compared to group I.

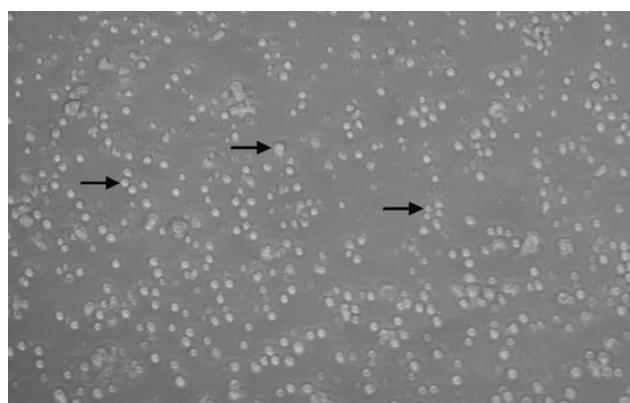


**Fig. 1:** A phase contrast micrograph of a primary culture of rat BM-MSCS on the 1st day of isolation and culture showing cultured cells (arrows) appearing rounded in shape, variable in size, crowded and floating. (Inverted microscope, x 200)

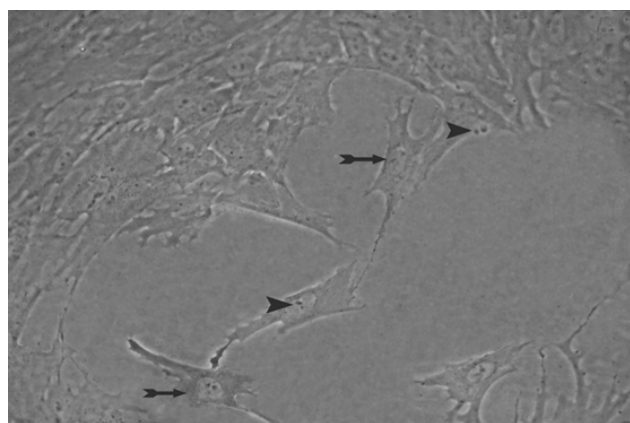


**Fig. 2:** A phase contrast micrograph of a primary culture of rat BM-MSCS on the 9th day showing fibroblast-like cells (bifid arrows) with long processes, central vesicular nuclei and prominent nucleoli (arrow heads). (Inverted microscope, x 200)

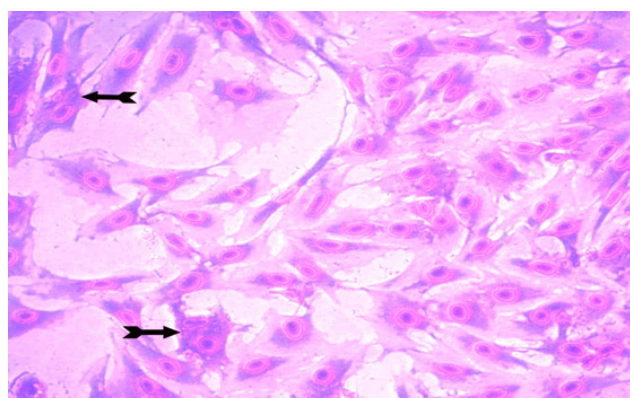


**Fig. 3:** A phase contrast micrograph of a primary culture of rat BM-MSCS stained with Giemsa stain showing star shaped adherent cells (bifid arrows) having granular cytoplasm and bluish vesicular nuclei with prominent nucleoli. (Inverted microscope, x 200)

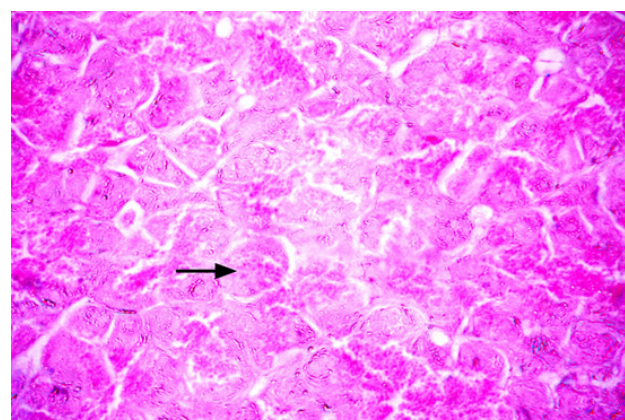


**Fig. 4:** A photomicrograph of rat pancreas from group I (control group) showing diffuse red pancreatic tissue without any blue reactivity for the Prussian blue. (Prussian blue stain, x 1000)

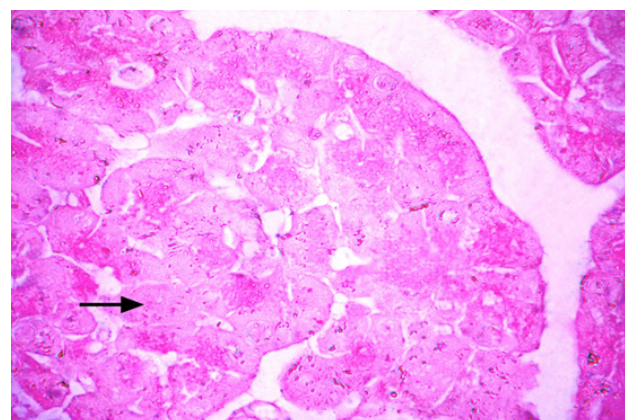


**Fig. 5:** A photomicrograph of rat pancreas from group II (acute pancreatitis group) showing diffuse red pancreatic tissue without any blue reactivity for the Prussian blue. (Prussian blue stain, x 1000)

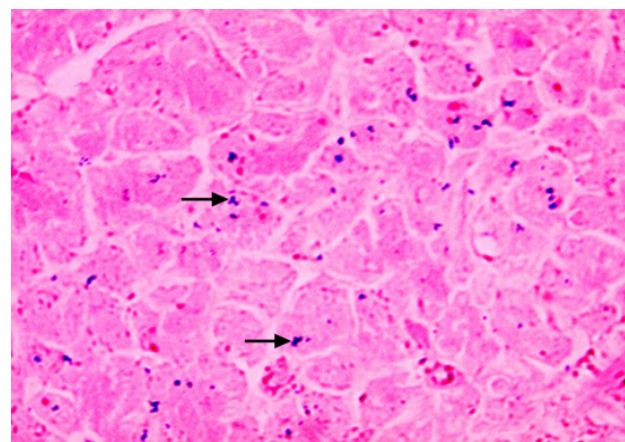


**Fig. 6:** A photomicrograph of rat pancreas from group III (BM-MSC treated group) showing blue dots of Prussian blue stain inside the acinar cells within the red pancreatic tissue (arrows). (Prussian blue stain, x 1000)

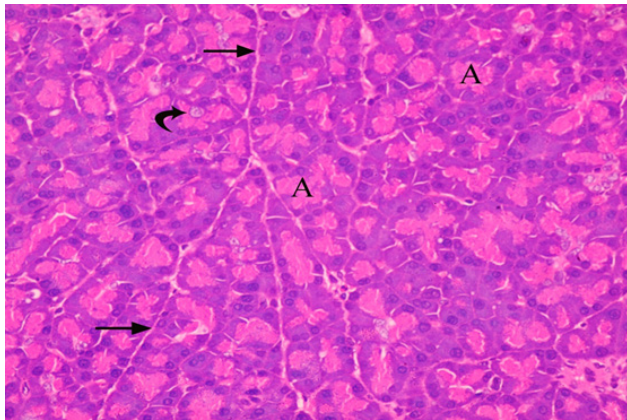


**Fig. 7:** A photomicrograph of rat pancreas from group I (control group) showing parts of pancreatic lobules with closely packed secretory acini (A). Notice the narrow spaces in between the pancreatic lobules (arrows). Also, nuclei of centroacinar cells are seen inside the lumen of some acini (curved arrows). (H&E x 400)

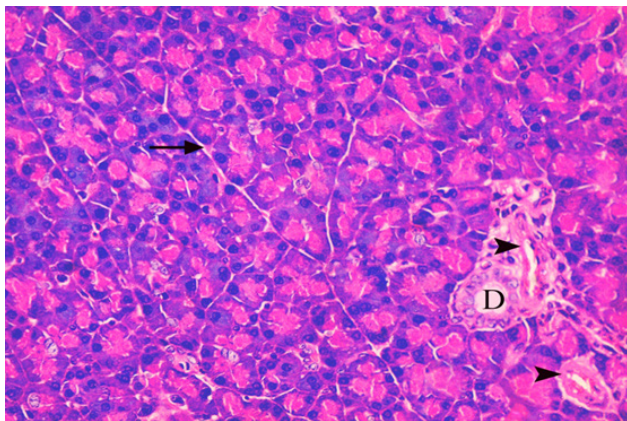


**Fig. 8:** A photomicrograph of rat pancreas from group I showing an intralobular duct (D) lined with simple cuboidal epithelium. Also, small blood vessels are seen (arrow heads). Notice thin septa separating the pancreatic lobules (arrow). (H&E x 400)

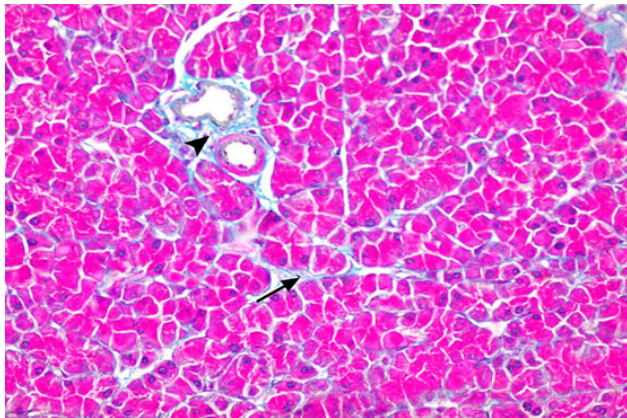


**Fig. 9:** A photomicrograph of rat pancreas from group I showing minimal amount of fine blue-stained collagen fibers around the blood vessels and interlobular ducts (arrow head) and in between the pancreatic lobules (arrow). (Masson's trichrome stain, x 400)

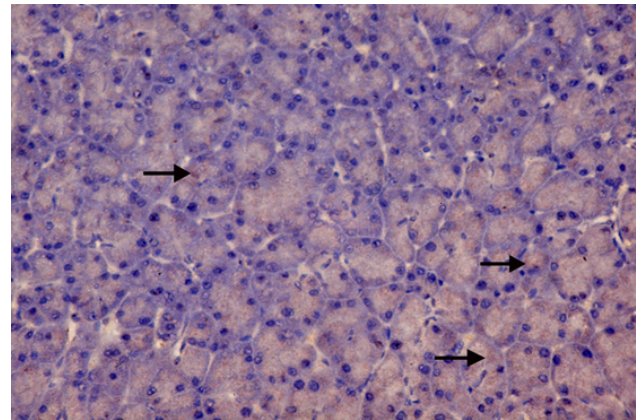


**Fig. 10:** A photomicrograph of rat pancreas from group I showing a weak positive cytoplasmic brownish reaction for caspase-3 in few acinar cells (arrows). (Caspase-3 immunoreaction counterstained with Hx, x 400)

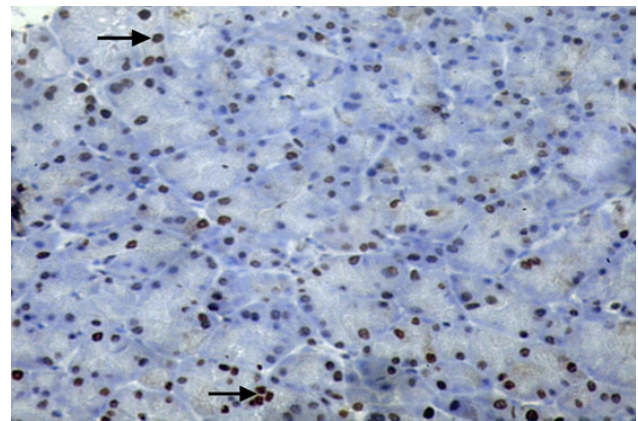


**Fig. 11:** A photomicrograph of rat pancreas from group I showing few acinar cells with positive nuclear brownish reaction for PCNA (arrows). (PCNA immunoreaction counterstained with Hx, x 400)

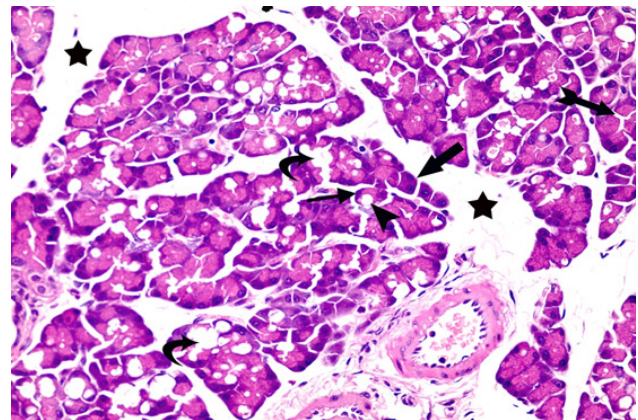


**Fig. 12:** A photomicrograph of rat pancreas from group II showing wide interlobular spaces (stars). In addition, some acini are disorganized and partially destroyed (curved arrows) and some acinar cells appear widely separated from each other (bifid arrow). Also, some cells show large cytoplasmic vacuoles (arrow head) with peripheral flattened nuclei (thin arrow). Notice dark basophilic cytoplasm of some acinar cells (thick arrow). (H&E x 400)

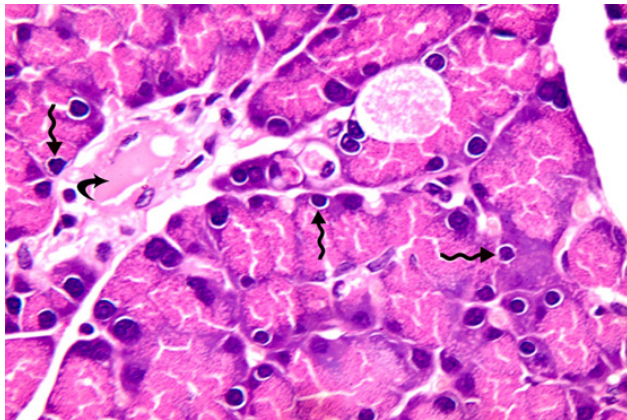


**Fig. 13:** A photomicrograph of rat pancreas from group II showing lysis of some acinar cells with appearance of homogenous acidophilic material (curved arrow). Notice small dark nuclei with perinuclear halos in some acinar cells (zigzag arrows). (H&E x 1000)

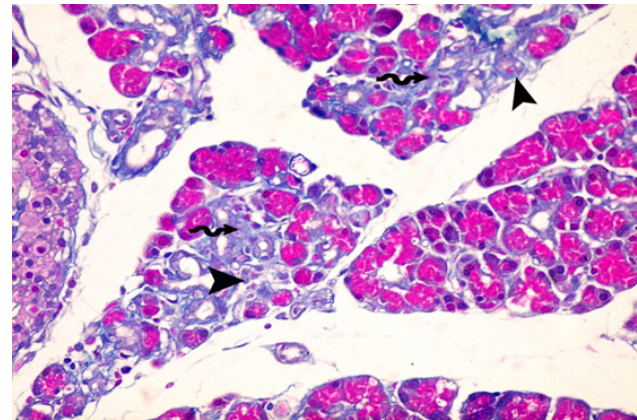


**Fig. 16:** A photomicrograph of rat pancreas from group II showing increased deposition of blue-stained collagen fibers inside the lobules in between the acini (zigzag arrows). Notice that some acini are replaced by collagen fibers (arrow heads). (Masson's trichrome stain, x 400)

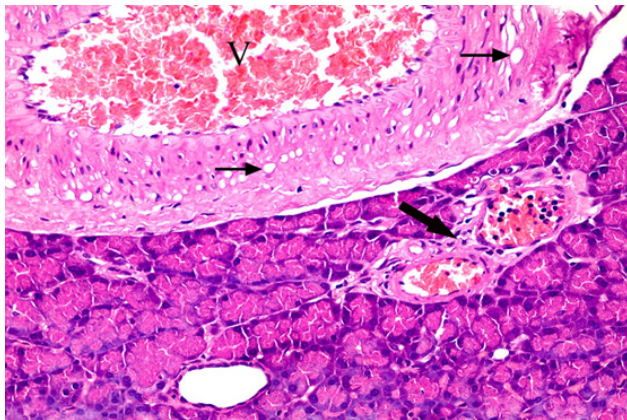


**Fig. 14:** A photomicrograph of rat pancreas from group II showing dilation and congestion of blood vessels (V) with thickening and vacuolation of tunica media of their wall (thin arrows). Notice inflammatory cells around the blood vessels (thick arrow). (H&E x 1000)

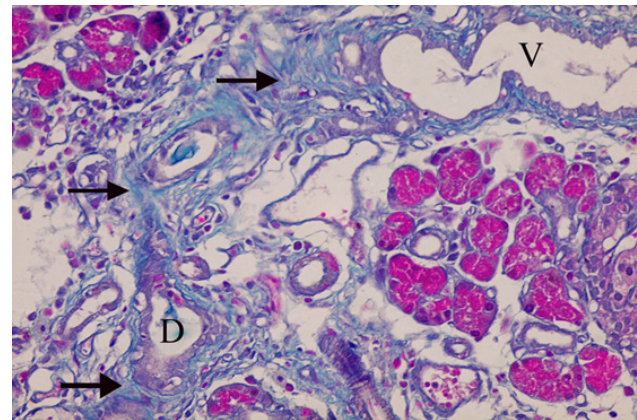


**Fig. 17:** A photomicrograph of rat pancreas from group II showing increased deposition of blue-stained collagen fibers (arrows) in the interlobular spaces around the dilated blood vessels (V) and interlobular ducts (D). (Masson's trichrome stain, x 400)

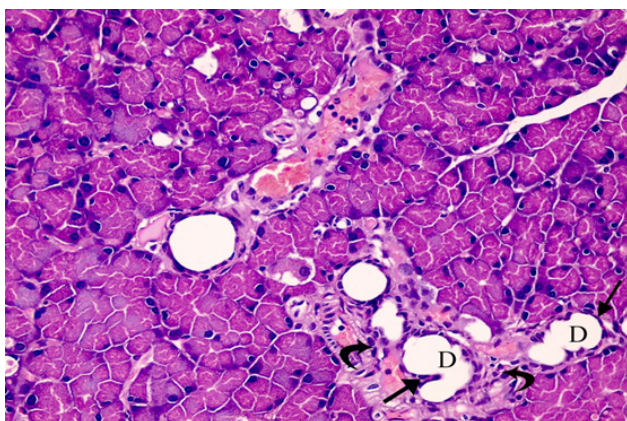


**Fig. 15:** A photomicrograph of rat pancreas from group II showing irregular interlobular ducts (D) with flattened lining epithelial cells (arrows). Notice mononuclear inflammatory cells surrounding the ducts (curved arrow). (H&E x 400)

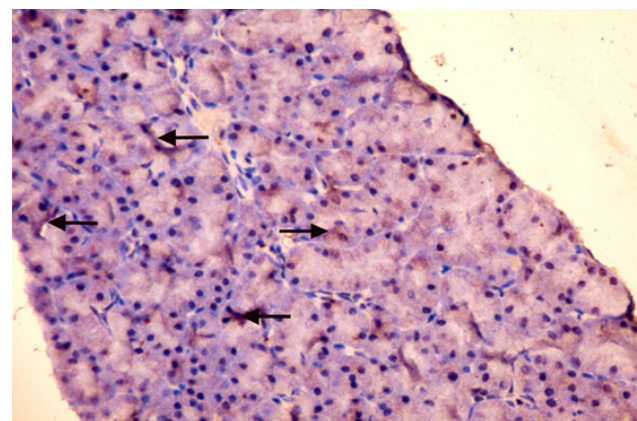


**Fig.18:** A photomicrograph of rat pancreas from group II showing an intense positive cytoplasmic brownish reaction for caspase-3 in many acinar cells (arrows). (Caspase-3 immunoreaction counterstained with Hx, x 400)

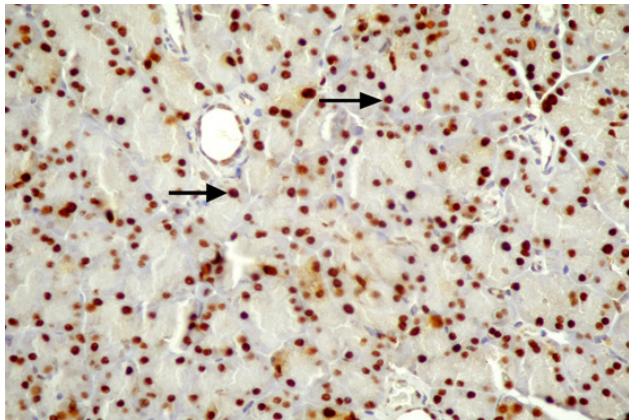


**Fig. 19:** A photomicrograph of rat pancreas from group II showing many acinar cells with positive nuclear brownish reaction for PCNA (arrows). (PCNA immunoreaction counterstained with Hx, x 400)

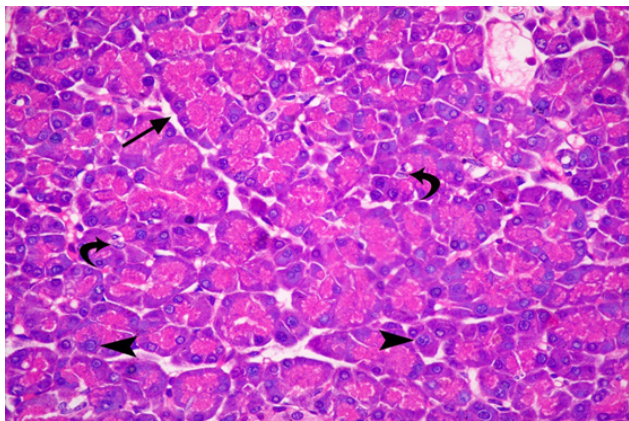


**Fig. 20:** A photomicrograph of rat pancreas from group III showing normal pancreatic architecture with narrow interlobular spaces (arrow). The acinar cells have basal cytoplasmic basophilia, apical acidophilia and their nuclei are rounded and basally located (arrow heads). Nuclei of centroacinar cells are seen in the lumen of some acini (curved arrows). (H&E x 400)

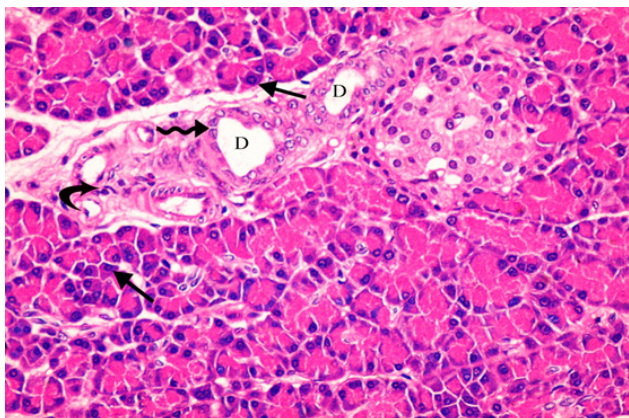


**Fig. 21:** A photomicrograph of rat pancreas from group III showing that few acinar cells show dark basophilic cytoplasm (thin arrows). The ducts (D) appear more or less normal and are lined by a single layer of cuboidal cells (zigzag arrow). Notice few inflammatory cells around the ducts (curved arrow). (H&E x 400)

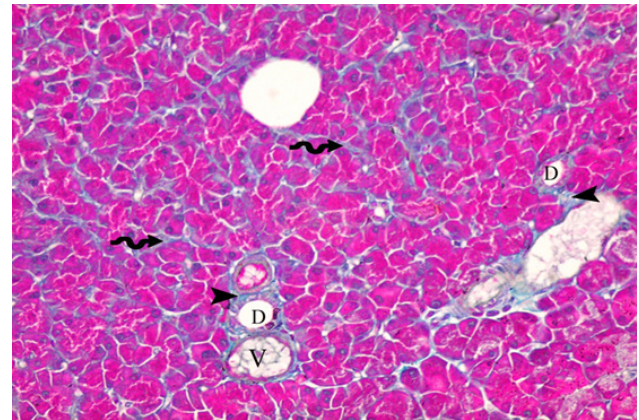


**Fig. 22:** A photomicrograph of rat pancreas from group III showing minimal amount of blue-stained collagen fibers in between the acini (zigzag arrows) as well as in the interlobular spaces (arrow heads) around the blood vessels (V) and interlobular ducts (D). (Masson's trichrome stain, x 400)

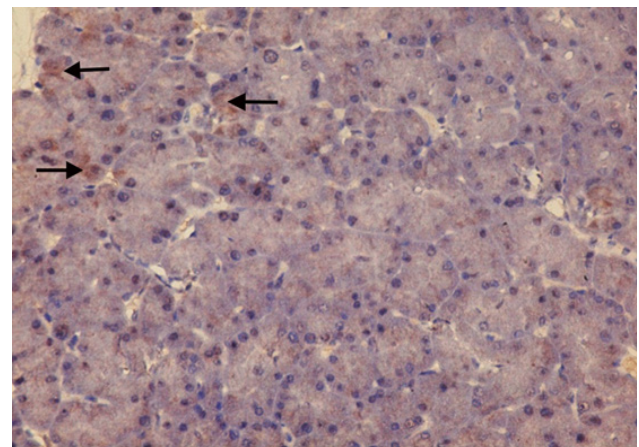


**Fig. 23:** A photomicrograph of rat pancreas from group III showing a weak positive cytoplasmic brownish reaction for caspase-3 in some acinar cells (arrows). (Caspase-3 immunoreaction counterstained with Hx, x 400)

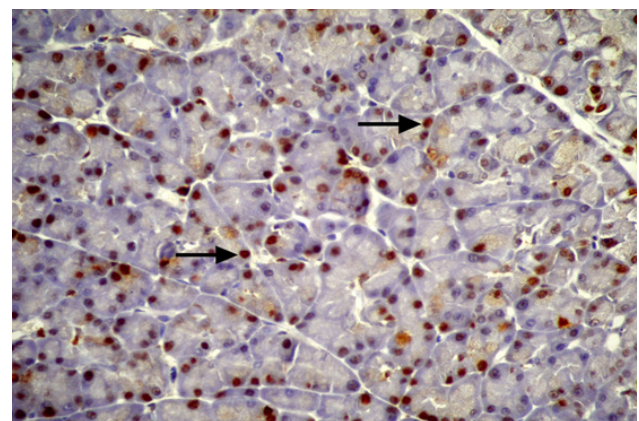


**Fig. 24:** A photomicrograph of rat pancreas from group III showing some acinar cells with positive nuclear brownish reaction for PCNA (arrows). (PCNA immunoreaction counterstained with Hx, x 400)

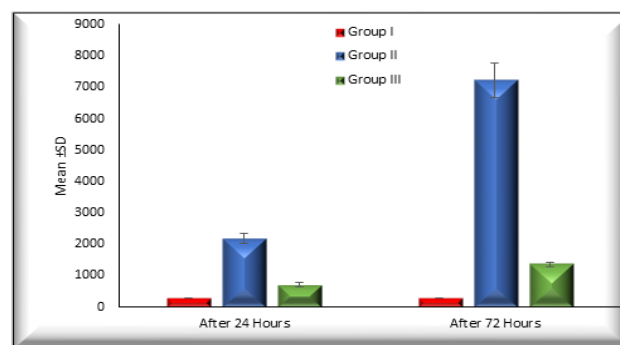
**Table 1:** The mean value of serum amylase level in the experimental groups at 24 hours and 72 hours

Groups	At 24 hours	At 72 hours
Group I	285.933±15.549 U/L	278.933±10.103 U/L
Group II	2193.500±157.552 U/L**	7230.200±541.422 U/L**
Group III	703.200±75.186 U/L*#	1367.733±71.773 U/L*#

\*\* Highly significant increase when compared with group I.

\* Significant increase when compared with group I.

# Significant decrease when compared with group II.



**Bar chart 1:** Comparison between the mean value of serum amylase level in the experimental groups at 24 hours and 72 hours

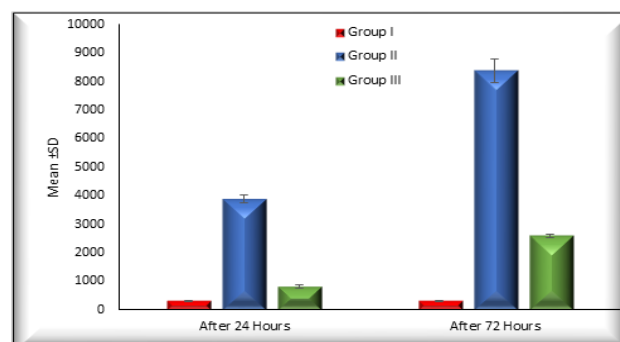
**Table 2:** The mean value of serum lipase level in the experimental groups at 24 hours and 72 hours

Groups	At 24 hours	At 72 hours
Group I	298.667±15.267 U/L	291.867±10.967 U/L
Group II	3889.800±132.348 U/L**	8381.900±398.081U/L**
Group III	801.800±62.229 U/L*#	2590.267±62.281U/L*#

\*\* Highly significant increase when compared with group I.

\* Significant increase when compared with group I.

# Significant decrease when compared with group II.



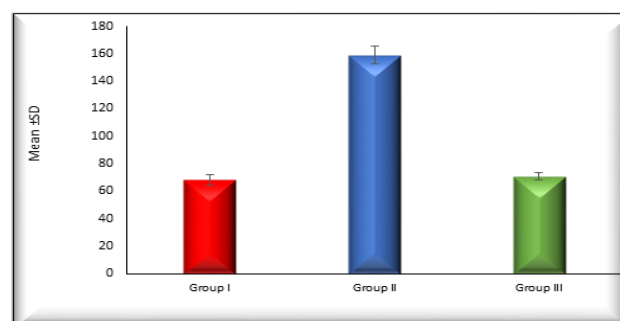
**Bar chart 2:** Comparison between the mean value of serum lipase level in the experimental groups at 24 hours and 72 hours

**Table 3:** The mean value of the area percentage of collagen fibres in sections stained with Masson's trichrome in the experimental groups

Groups	Mean value of area percentage of collagen fibres
Group I	67.879±3.842
Group II	158.999±6.266*
Group III	70.795±2.386#

\* Significant increase when compared to group I.

# Significant decrease when compared to group II.



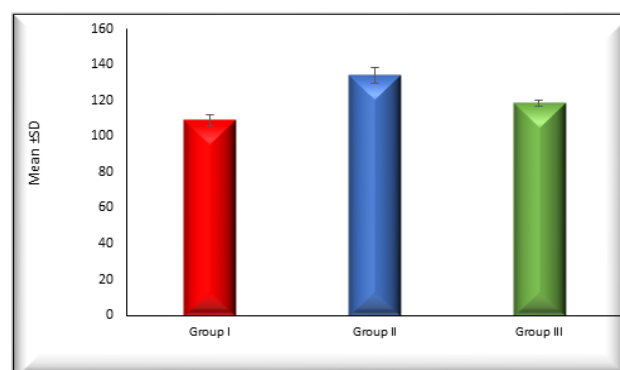
**Bar chart 3:** Comparison between the mean value of area percentage of collagen fibers in the experimental groups in Masson's trichrome stained sections

**Table 4:** The mean value of color density of caspase-3 immunoreactivity of experimental groups

Groups	Mean value of color density of caspase-3 immunoreactivity
Group I	109.000±3.229
Group II	134.100±4.433*
Group III	111.667±2.160#

\* Significant increase when compared to group I.

# Significant decrease when compared to group II.



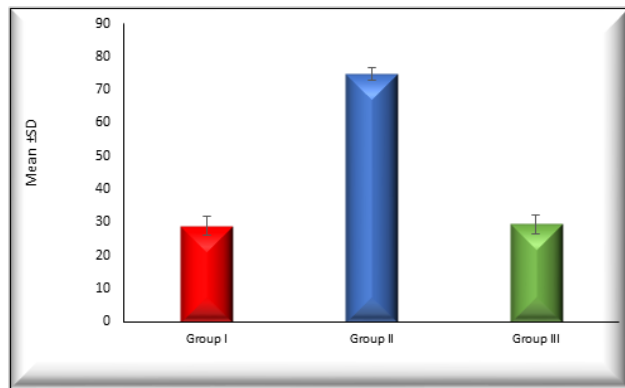
**Bar chart 4:** Comparison between the mean value of color density of caspase-3 immunoreactivity of the experimental groups

**Table 5:** The mean value of PCNA-Labeling Index immunoreactivity of control and experimental groups

Groups	Mean values of PCNA-Labeling Index immunoreactivity
Group I	28.963±2.756
Group II	74.752±1.869*
Group III	29.441±2.885#

\* Significant increase when compared to group I.

# Significant decrease when compared to group II.



**Bar chart 5:** Comparison between the mean value of PCNA-Labeling Index immunoreactivity of the experimental groups

## DISCUSSION

Acute pancreatitis (AP) is one of the most frequent gastrointestinal disorders, requiring hospitalisation<sup>[29]</sup>. Induction of acute pancreatitis using L-arginine is considered one of the most accepted models of AP as it produces biochemical and histological changes in the pancreas resembling those in humans<sup>[30]</sup>. According to Moreira *et al.* (2011) and Zhan *et al.* (2016)<sup>[31,32]</sup>, the peak of the histological changes occurs around 72 hours after the induction of AP, so in this work sacrifice of rats was done on the 4<sup>th</sup> day from AP induction.

In the last 25 years, the use of mesenchymal stem cells (MSCs) for tissue repair in acute diseases has expanded dramatically. MSC infusion has been demonstrated to be helpful in a variety of models of acute injury. Their relative ease of access as well as their ability to modulate the immune system, to migrate to sites of tissue injury and to repair tissue together with their antifibrotic activity have made them an attractive cell source for many cell therapy approaches<sup>[33,34]</sup>.

In the present study, biochemical analysis of blood samples obtained from rats of group II (AP group) confirmed the induction of AP as it showed a highly significant increase of both serum amylase and lipase levels 24 hours and 72 hours after administration of L-arginine as compared to group I (control group). These findings were in accordance with the results of Abd El-Rahman *et al.* (2011) and Chen *et al.* (2012) in their studies on AP<sup>[35,36]</sup>.

Matull *et al.* (2006) and Meher *et al.* (2015)<sup>[37,38]</sup> illustrated that amylase activity rises quickly within the first 12 hours after induction of AP and remains elevated for three to five days before finally being excreted by the kidneys. On the other hand, Basnayake and Ratnam (2015)<sup>[39]</sup> documented that the serum lipase level increases within 3-6 hours after induction of AP then peaks at 24 hours and remains elevated for 8-14 days owing to its significant reabsorption by the renal tubules, so it remains at a high concentration for a long period.

In this regard, Cornett *et al.* (2011) and Hasan *et al.* (2015)<sup>[40,41]</sup> attributed the increased levels of pancreatic enzymes in AP to uncontrolled production of free radicals that directly attack the lipids and proteins in the membranes of zymogen granules, disrupting the permeability of secretory granules and resulting in the diffusion of a large amount of pancreatic enzymes into the pancreatic interstitial tissue.

In the present work, light microscopic examination of pancreatic specimens obtained from rats of group II (AP group) revealed loss of the normal architecture of the pancreas with evident histological changes in its exocrine portion in the form of widely separated lobules and irregular disorganized widely separated acini. A similar finding was previously observed by Ali *et al.* (2013)<sup>[41]</sup> and attributed this change to pancreatic edema which occurs due to increased production of hyaluronic acid with its hydrophilic property resulting in attraction and accumulation of water in the interstitial tissues. Another explanation was demonstrated by Aziz *et al.* (2017)<sup>[42]</sup> who attributed the pancreatic tissue edema to increased vascular permeability secondary to overproduction of nitric oxide (NO) caused by increased nitric oxide synthase enzyme activity (NOS) as a part of the condition of oxidative stress.

Nasr *et al.* (2019)<sup>[22]</sup> observed many histological findings in their study on AP in the form of disorganized acinar architecture. Bhattacharyya *et al.* (2014) as well as Soliman *et al.* (2019)<sup>[43,44]</sup> explained these degenerative findings are to be due to oxidative stress and the production of reactive oxygen species (ROS), which have a direct harmful effect on pancreatic acinar cells. The ROS production increases during inflammatory conditions, radiation, metabolism of drugs and environmental toxins.

The present work also showed homogenous acidophilic material in between the pancreatic lobules in animals of group II (AP group). This finding was in accordance with Kumar *et al.* (2018)<sup>[45]</sup> who attributed this change to be due to degenerative changes and necrosis which develop secondary to the effects of ROS on both the cell membrane and the organelles membranes leading to leakage of the lysosomal enzymes into the cytoplasm causing digestion and degradation of all cellular contents.

In the present work, group II (AP group) showed that many acinar cells appeared separated from each other. This was in agreement with Rao (2008)<sup>[46]</sup> who explained this finding due to disruption of tight junctions, zonula adherens and cytoskeleton as well as impaired function of the intercellular proteins through protein modification in cell membranes secondary to cellular damage by the ROS.

The multiple cytoplasmic vacuoles with partially degraded material within the pancreatic acinar cells were also reported by Gukovsky and Gukovskaya (2010)<sup>[47]</sup> who suggested that these vacuoles are the consequence of defective autophagy, which is caused by an imbalance between cathepsin L (CatL) (which destroys trypsinogen and trypsin) and cathepsin B (CatB) (which converts

trypsinogen to trypsin), resulting in intra-acinar buildup of active trypsin.

The dark basophilic cytoplasm of some acinar cells was previously observed by Zhang *et al.* (2014)<sup>[48]</sup> and attributed this finding to be due to apoptosis and accumulation of small round basophilic bodies of autolysosomes in the acinar cells resulting in basophilic cytoplasmic condensation.

Regarding nuclear pyknosis, Hyvonen *et al.* (2006) and Soliman *et al.* (2015)<sup>[49,50]</sup> proposed that excessive ROS production could cause severe damage to cellular macromolecules, particularly DNA, via mitochondrial dysfunction, resulting in the activation of apoptogenic proteases and endonuclease activation secondary to ATP depletion, resulting in the fragmentation of chromatin into short segments and the appearance of nuclear pyknosis.

Mononuclear inflammatory cells were detected within the pancreatic lobules between the acini and in the interlobular spaces surrounding blood vessels and ducts in the current study. Similar findings were observed by Wang *et al.* (2017)<sup>[51]</sup> in their studies on AP. They explained this inflammatory infiltration to be due to injury of pancreatic acinar cells with subsequent release of many pro-inflammatory factors such as TNF- $\alpha$ , IL-1 $\beta$  and IL-6 which promote migration and accumulation of inflammatory cells (including neutrophils and macrophages) in the pancreas.

The present work showed that most of the blood vessels in group II (AP group) appeared dilated and congested with thickening and irregularity of their walls as well as vacuolation of the tunica media layer within the walls of dilated blood vessels. This was in agreement with the results of Elbakary and Bayomy (2011)<sup>[52]</sup> stated that these alterations were caused by an excess of nitric oxide (NO), a calming substance produced from the endothelium that is a highly reactive free radical. It is a significant role in both systemic and local hemodynamic disturbances since it has the ability to generate vasodilation and hypotension.

In line with these observations, vacuolation of the tunica media layer within the walls of dilated blood vessels was previously documented by Mansfield (2012) and Polydorides (2019)<sup>[53,54]</sup>. They explained it to be due to release of activated trypsin which stimulates the activation of other proteases such as elastase, lipase and chymotrypsin. Elastase degrades elastin in blood vessel walls leading to vasculitis. Lipase causes fat hydrolysis leading to fat necrosis especially around the pancreas and chymotrypsin stimulates the formation of ROS. In addition, Adiguzel *et al.* (2014)<sup>[55]</sup> stated that ROS are known to be involved in extracellular matrix degradation and can cause apoptosis of smooth muscle cells (SMCs) lining blood vessels, resulting in vessel wall degeneration, dilatation, and vacuolation.

The present work also showed that the interlobular ducts were dilated with irregularity and disruption of their walls and some ducts were lined with flattened epithelial cells in AP group. Similar findings were also reported by Abdel Wahab *et al.* (2017) and Rizk *et al.* (2017)<sup>[56,57]</sup>

who attributed these changes to the release of digestive and lysosomal enzymes from the acinar cells. These enzymes cause inflammation to the cells of pancreatic ducts, limitations of pancreatic regeneration, pancreatic duct obstruction and consequently dilatation of the ducts. Moreover, Nolte *et al.* (2016) and Aziz *et al.* (2017)<sup>[58,42]</sup> suggested that the flattened epithelial cells lining some interlobular ducts may be due to dilation of interlobular ducts with cystic formation resulting in downgrowth of entrapped surface mucosa and flattened lining epithelial cells.

As regards Masson's trichrome-stained sections obtained from AP group, the present work demonstrated enhanced collagen fibre deposition between the acini and in the interlobular regions surrounding dilated blood arteries and dilated ducts. This result was in agreement with the results of Sadek and Khattab (2017) and Elbassuoni and Abdel Hafez (2019)<sup>[59,60]</sup> in their studies on AP. They suggested that the release of free radicals could activate the pancreatic stellate cells and stimulate their proliferation and differentiation to myofibroblast-like cells which are capable of production of extracellular matrix components resulting in deposition of excess collagen fibers.

As regards the immunohistochemical reaction in AP group, caspase-3 immunostained sections in the present study showed a significant increase in the mean color density of caspase-3 immunoreaction in the cytoplasm of most of pancreatic acinar cells. This came in agreement with Robles *et al.* (2015)<sup>[25]</sup> who studied the presence of cleaved caspase-3 in AP to evaluate apoptotic cells. Abdel Wahab *et al.* (2017)<sup>[56]</sup> stated in their study on the pancreas that cleaved caspase-3 is considered an important marker of apoptosis being responsible for proteolytic cleavage of a large number of proteins, DNA fragmentation and nuclear shrinkage during apoptosis.

Additionally, PCNA immunostained sections from the AP group demonstrated a high number of acinar cells with a positive nuclear brownish response and a substantial increase in PCNA-LI. This finding could be explained by the reports of Strobel *et al.* (2010)<sup>[61]</sup> he reported that apoptotic cells produce chemokines that activate pancreatic duct cells. The latter were thought to be a pancreatic stem cell niche that promotes pancreatic inflammation-induced proliferation.

The present work showed that treatment with BM-MSCs in group III significantly reduced the pancreatic injury, alleviated the histological changes and Reduced levels of amylase serum and lipase. These findings were in accordance with Yin *et al.* (2015)<sup>[62]</sup> who has shown significant reduction of serum amylase and lipase levels after treatment with BM-MSCs in their study on the role of BM-MSCs on AP. Tu *et al.* (2012) and Qu *et al.* (2017)<sup>[63,64]</sup> attributed this improvement in the biochemical parameters to be due to the ability of MSCs to differentiate into the pancreatic cells after homing in the pancreas.

Qian *et al.* (2015)<sup>[65]</sup> illustrated that migration of the iron-labeled BM-MSCs to the damaged pancreatic tissues occurs gradually then peaking on the fifth to seventh days after injection. Also, Ahmed-Sorour and Abd-Elgalil (2019)<sup>[66]</sup> could detect the iron labeled BM-MSCs in the renal tissue using Prussian blue stain and reported that MSCs are able to engraft into renal tissue and repair the affected cells.

As regards hematoxylin and eosin-stained pancreatic sections obtained from BM-MSCs treated group, the present work showed improvement with apparent preservation of the normal pancreatic architecture of pancreatic lobules and acini. These findings came in accordance with Schneider and Saur (2011) and Zhao *et al.* (2016)<sup>[67,68]</sup> who studied the effect of MSCs on AP. They reported that acinar cells degeneration and pancreatic edema were significantly reduced after BM-MSCs transplantation. These findings could be explained by the reports of Tu *et al.* (2012) and Yin *et al.* (2015)<sup>[63,62]</sup> who illustrated that the beneficial effects of BM-MSCs in treatment of AP are mediated through a paracrine effect on the surrounding acini by regulating the oxidative stress levels and inhibiting the extensive release of mediators of inflammation and cytokines.

Regarding Masson's trichrome-stained sections obtained from BM-MSCs treated group, the present work showed relative decreased deposition of collagen fibers in specimens when compared to acute pancreatitis group. This result was in agreement with Moustafa *et al.* (2020)<sup>[69]</sup> who studied the effect of MSCs in relieving the pancreatic fibrosis. They observed that MSCs decreased excessive extracellular matrix production and breakdown during fibrosis, as well as collagen deposition, which is a major component of the extracellular matrix, resulting in a reduction in pancreatic fibrosis.

Regarding the immunohistochemical-stained sections obtained from BM-MSCs treated group, the current work showed that caspase-3 immunostained sections revealed a weak positive cytoplasmic brownish reaction when compared to acute pancreatitis group. Similarly, Ahmed *et al.* (2018)<sup>[70]</sup> found that MSCs have an antiapoptotic effect on the acinar cells through secretion of some antiapoptotic mediators such as chemokine XCL1 that acts on the injured cells making them more resistable to apoptosis. Also, PCNA immunostained sections from BM-MSCs-treated group showed few acinar cells with positive nuclear reaction when compared to acute pancreatitis group. This finding was parallel to the results of Huh *et al.* (2018)<sup>[71]</sup> who observed decreased expression of PCNA in the group treated with MSCs after acute lung injury and explained it as MSCs can partially suppress and regulate cellular proliferation. Moreover, Haroun *et al.* (2020)<sup>[72]</sup> demonstrated that the decreased proliferation rate observed with BM-MSCs is due to MSCs' antioxidant activity.

## CONCLUSION

From the previous data, After induction of acute pancreatitis, it was discovered that BM-MSCs had a

substantial ameliorative therapeutic effect on exocrine pancreatic tissue. This effect was confirmed by biochemical, histological and immunohistochemical methods.

## CONFLICT OF INTERESTS

There are no conflicts of interest.

## REFERENCES

1. Saljoughian M. Acute pancreatitis: A medical emergency. *U.S. Pharmacist Journal* 2014; 39(12): 1-9.
2. El-Ashmawy NE, Khedr NF, El-Bahrawy HA and Hamada OB. Anti-inflammatory and antioxidant effects of captopril compared to methylprednisolone in L-arginine-induced acute pancreatitis. *Digestive Diseases and Sciences Journal* 2018; 63: 1497–1505.
3. Abdelzaher WY, Ahmed SM, Welson NN, Marraiki N, Batiha GE and Kamel MY. Vinpocetine ameliorates L-arginine induced acute pancreatitis via Sirt1/Nrf2/TNF pathway and inhibition of oxidative stress, inflammation, and apoptosis. *Biomedicine and Pharmacotherapy Journal* 2020; 133: 1-8.
4. Hasan MI, Bakr AG and Shalkami AG. Modulation of L-arginine-induced acute pancreatitis by meloxicam and/or L-carnitine in rats. *International Journal of Basic and Clinical Pharmacology* 2015; 4(6): 1247-1253.
5. Ragy MM, Ali FF and Toni ND. Comparing the preventive effect of sodium hydrosulfide, leptin, and curcumin against L-arginine induced acute pancreatitis in rats: Role of corticosterone and inducible nitric oxide synthase. *Endocrine Regulations Journal* 2019; 53(4): 221-230.
6. Magnus T, Liu y, Parker GC and Rao MS. Stem cell myths. *Philosophical Transaction of the Royal Society B Journal* 2008; 363(1489): 9-22.
7. Chou YH, Pan SY, Yang CH and Lin SL. Stem cells and kidney regeneration. *Journal of Formosan Medical Association* 2014; 113: 201-209.
8. Berebichez-Fridman R and Montero-Olvera PR. Sources and clinical applications of mesenchymal stem cells. *Sultan Qaboos University Medical Journal* 2018; 18(3): 264-277.
9. Hmadcha A, Martin-Montalvo A, Gauthier BR, Soria B and Capilla-Gonzalez V. Therapeutic potential of mesenchymal stem cells for cancer therapy. *Frontiers in Bioengineering and Biotechnology Journal* 2020; 8(43): 1-13.
10. Papadimitriou N, Li S and Henriksson HB. Iron Sucrose-labeled human mesenchymal stem cells: In *vitro* multilineage capability and in *vivo* traceability in a lapine xenotransplantation model. *Stem Cells and Development Journal* 2015; 24(20): 2403-2412.

11. Ferrari E and Soloviev M. In *Vitro* Labeling Mesenchymal Stem Cells with Superparamagnetic Iron Oxide Nanoparticles: Efficacy and Cytotoxicity. (Ch.18). In: Nanoparticles in Biology and Medicine Methods and Protocols. 2nd edition. Springer, New York. 2020; pp. 235-250.
12. National Research Council of the National Academies. Environment, Housing and Management. (Ch.3). In: Guide for the Care and Use of Laboratory Animals. 8th edition. National Academies Press, Washington, D.C. 2011; pp. 41-104.
13. Dawra R and Saluja AK. L-arginine-induced experimental acute pancreatitis. The pancreapedia Journal 2012; 1: 1-8.
14. Dong H, Tan X, Fu M, Zhao J, Ge Q, Chen Y and Li Y. Experimental study on bone marrow mesenchymal stem cells for the treatment of acute pancreatitis in rats. MOJ Applied Bionics and Biomechanic 2018; 2(1): 1-7.
15. Kawakubo K, Ohnishi S, Kuwatani M and Sakamoto N. Mesenchymal stem cell therapy for acute and chronic pancreatitis. Journal of Gastroenterology 2018; 53:1-5.
16. Huo L, Shi W, Chong L, Wang J, Zhang K and Li Y. Asiatic acid inhibits left ventricular remodeling and improves cardiac function in a rat model of myocardial infarction. Experimental and Therapeutic Medicine Journal 2016; 11(1): 57-64.
17. Gneechi M and Melo L. Bone marrow-derived mesenchymal stem cells: isolation, expansion, characterization, viral transduction and production of conditioned medium. Methods Mol Biol Journal 2009; 482: 281-294.
18. McFarlin K, Gao X, Liu Y, Dulchavsky D, Kwon D, Arbab A, Bansal M, Li Y, Chopp M, Dulchavsky S and Gautam S. Bone marrow-derived mesenchymal stromal cells accelerate wound healing in the rat. Wound repair and regeneration Journal 2006; 14(4): 471-478.
19. Nardi NB and Meirelles LS. Mesenchymal Stem Cells: Isolation, In *Vitro* Expansion and Characterization. (Ch.11). In: Handbook of Experimental Pharmacology: Stem Cells. Wobus AM and Boheler KR (eds.). 174<sup>th</sup> edition. Springer, Verlag, Berlin, Heidelberg. 2008; pp. 249-282.
20. Hany E, Sobh MA, Abou ElKhier MT, ElSabaa HM and Zaher AR. The effect of different routes of injection of bone marrow mesenchymal stem cells on parotid glands of rats receiving cisplatin: A comparative study. International Journal of Stem Cells 2017; 10(2): 169-178.
21. Wang L, Chen L, Wang Q, Wang L, Wang H, Shen Y, Li X, Fu Y, Shen Y and Yu Y. Circulating endothelial progenitor cells are involved in VEGFR-2-related endothelial differentiation in glioma. Oncology Reports Journal 2014; 32(5): 2007-2014.
22. Nasr SE, Radwan DM, Aboulkhair AG and Hamed MM. Comparative histological study on the effect of bone marrow derived mesenchymal stem cells versus wheat germ oil on acute pancreatitis in a rat model. Egyptian Journal of Histology 2019; 42(3): 540-553.
23. Bancroft JD and Layton C. The Hematoxylin and Eosin. (Ch.10). In: Bancroft's Theory and Practice of Histological Techniques. Suvarna SK, Layton C and Bancroft JD (eds.). 8th edition. Elsevier, China. 2019a; pp. 126-138.
24. Bancroft JD and Layton C. Connective and Other Mesenchymal Tissues with Their Stains. (Ch.12). In: Bancroft's Theory and Practice of Histological Techniques. Suvarna SK, Layton C and Bancroft JD (eds.). 8th edition. Elsevier, China. 2019b; pp. 153-175.
25. Robles L, Vaziri ND, Li S, Takasu C, Masuda Y, Vo K, Farzaneh SH, Stamos MJ and Ichii H. Dimethyl fumarate ameliorates acute pancreatitis in rodent. Pancreas Journal 2015; 44(3): 441-447.
26. El-kott AF, Kandeel AA, Abdel El-Aziz SF and Ribea HM. Anti-tumor effects of bee honey on PCNA P53 expression in the rat hepatocarcinogenesis. International Journal of Cancer Research 2012; 8: 130-139.
27. Mousa AM. Histological and immunohistochemical study on the effect of polyhexanide-preserved contact lens solution on albino rat cornea and the possible protective role of carboxymethylcellulose. Egyptian Journal of Histology 2010; 33(2): 288-300.
28. Davies HT and Crombie LK. What are Confidence Intervals and P-values?. 2nd edition, Hayward Group Ltd, London. 2009; pp. 1-6.
29. Marzaban R. A glance at acute pancreatitis (AP). Gastroenterology and Hepatology Journal 2017; 7(2): 1-5.
30. Dawra R, Sharif R, Phillips P, Dudeja V, Dhau lakhandi D and Saluja AK. Development of a new mouse model of acute pancreatitis induced by administration of L-arginine. American Journal of Physiology Gastrointestinal and Liver Physiology 2007; 292(4): 1009-1018.
31. Moreira M, Matias JE, De Souza CJ, Nicoluzzi JE, Caron PE and Repka JC. Action of tacrolimus in arginine induced experimental acute pancreatitis. Revista do Colegio Brasileiro de Cirurgioes Journal 2011; 38(4): 260-265.

32. Zhan X, Wang F, Bi Y and Ji B. Animal models of gastrointestinal and liver diseases. Animal models of acute and chronic pancreatitis. *American Journal of Physiology Gastrointestinal and Liver Physiology* 2016; 311(3): 343-355.
33. Jung KH, Song SU, Yi T, Jeon MS, Hong SW, Zheng HM, Lee hS, Choi MJ, Lee DH and Hong SS. Human bone marrow-derived clonal mesenchymal stem cells inhibit inflammation and reduce acute pancreatitis in rats. *Gastroenterology Journal* 2011; 140(3): 998-1008.
34. Le Blanc K and Davies LC. MSCs-cells with many sides. *Cytotherapy Journal* 2018; 20(3): 273-278.
35. Abd El-Rahman AA, Mishriki ES, Shehab AA and Mona AA. Therapeutic effect of pentoxifylline versus losartan on experimentally induced acute pancreatitis in adult albino rats: Light and electron microscopic study. *Egyptian journal of Histology* 2011; 34 (3): 606-619.
36. Chen J, Cai QP, Shen PJ, Yan RL, Wang CM, Yang DJ, Fu HB and Chen XY. Netrin-1 protects against L-arginine-induced acute pancreatitis in mice. *PLOS One Journal* 2012; 7(9): 1-9.
37. Matull WR, Pereira SP and O'Donohue JW. Biochemical markers of acute pancreatitis. *Journal of Clinical pathology* 2006; 59(4): 340-344.
38. Meher S, Mishra TS, Sasmal PK, Rath S, Sharma R, Rout B and Sahu MK. Role of biomarkers in diagnosis and prognostic evaluation of acute pancreatitis. *Journal of Biomarkers* 2015; 2015: 519534.
39. Basnayake C and Ratnam D. Blood tests for acute pancreatitis. *Australian Prescriber Journal* 2015; 38(4): 128-130.
40. Cornett DD, Spier BJ, Eggert AA and Pfau PR. The causes and outcome of acute pancreatitis associated with serum lipase >10,000 U/L. *Digestive Diseases and Sciences Journal* 2011; 56: 3376-3381.
41. Ali M, Saleh H and Farghaly L. Role of thyroxin versus Brewer's yeast supplementation in amelioration of pancreatic alterations induced by hypothyroidism in adult male albino rats. *The Egyptian Journal of Histology* 2013; 36: 918-930.
42. Aziz NM, Kamel MY and Rifaai RA. Effects of hemin, a heme oxygenase-1 inducer in L-arginine-induced acute pancreatitis and associated lung injury in adult male albino rats. *Endocrine Regulations Journal* 2017; 51(1): 20-30.
43. Bhattacharyya A, Chattopadhyay R, Mitra S and Crowe SE. Oxidative stress: An essential factor in the pathogenesis of gastrointestinal mucosal diseases *Physiological Reviews Journal* 2014; 94(2): 329-354.
44. Soliman GF, Ibrahim W and Abdallah H. Therapeutic effect of L-carnitine on acute pancreatitis induced by L-arginine in rats: Possible role of beclin gene and inducible nitric oxide synthase. *Medical Journal of Cairo University* 2019; 87(3): 1793-1803.
45. Kumar V, Abbas AK and Aster JC. Cell Injury, Cell Death and Adaptations. (Ch.2). In: Robbins Basic Pathology. 10th edition. Elsevier, Philadelphia, Pennsylvania. 2018; pp. 31-56.
46. Rao R. Oxidative stress-induced disruption of epithelial and endothelial tight junctions. *Frontiers in Bioscience Journal* 2008; 13: 7210-7226.
47. Gukovsky I and Gukovskaya AS. Impaired autophagy underlies key pathological responses of acute pancreatitis. *Autophagy Journal* 2010; 6(3): 428-429.
48. Zhang L, Zhang J, Shea K, Xu L, Tobin G, Knapton A, Sharron S and Rouse R. Autophagy in pancreatic acinar cells in caerulein-treated mice: immunolocalization of related proteins and their potential as markers of pancreatitis. *Toxicologic pathology Journal* 2014; 42(2): 435-457.
49. Hyvonen MT, Herzig KH, Sinervirta R, Albrecht E, Nordback I, Sand J, Keinänen TA, Vepsäläinen J, Grigorenko N, Khomutov AR, Kruger B, Janne J and Alhonen L. Activated polyamine catabolism in acute pancreatitis: Alpha-methylated polyamine analogues prevent trypsinogen activation and pancreatitis-associated mortality. *American Journal of Pathology* 2006; 168(1): 115-122.
50. Soliman ME, Mahmoud BL, Kafafy MA, El Haroun HM and Mohamed DM. Histological changes in cornea following repeated exposure to benzalkonium chloride and the possible protective effect of topically applied sodium hyaluronate. *Nature and Science journal* 2015; 13(5): 161-171.
51. Wang N, Zhang F, Yang L, Zou J, Wang H, Liu K, Liu M, Zhang H, Xiao X and Wang K. Resveratrol protects against L-arginine-induced acute necrotizing pancreatitis in mice by enhancing SIRT1-mediated deacetylation of p53 and heat shock factor 1. *International Journal of Molecular Medicine* 2017; 40(2): 427-437.
52. Elbakary RH and Bayomy N. Histological and immunohistochemical study of the effect of orlistat on the exocrine pancreas of adult female albino rat. *Egyptian Journal of Histology* 2011; 34(2): 302-310.
53. Mansfield C. Pathophysiology of acute pancreatitis: Potential application from experimental models and human medicine to dogs. *Journal of Veterinary Internal Medicine* 2012; 26(4): 875-887.
54. Polydorides AD. Vasculitis. (Ch.6). In: Diagnostic Pathology: Gastrointestinal. Greenson JK (ed). Elsevier, Philadelphia. 2019; pp. 616-623.

55. Adiguzel Z, Arda N, Kacar O, Serhatli M, Tas SG, Baykal AT, Baysal K and Acilan C. Evaluation of apoptotic molecular pathways for smooth muscle cells isolated from thoracic aortic aneurysms in response to oxidized sterols. *Molecular Biology Reports Journal* 2014; 41(12): 7875-7884.
56. Abdel Wahab SA, Ali AH, Mahmoud AS and Abelhaleem AH. Effect of orlistat on the pancreas of the female albino rat: Histological and histochemical study. *Journal of Medical Histology* 2017; 1(1): 30-43.
57. Rizk AE, Abdel Fattaha S and El Sebaieb M. Can vitamin E protect the pancreas against ethanol-induced alterations in adult male albino rats? A histomorphometric and immunohistochemical study. *Kasr Al Ainy Medical Journal* 2017; 23: 43-53.
58. Nolte T, Brander-Weber P, Dangler C, Deschl U, Elwell MR, Greaves P, Hailey R, Leach MW, Pandiri AR, Rogers A, Shackelford CC, Spencer A, Tanaka T and Ward JM. Nonproliferative and proliferative lesions of the gastrointestinal tract, pancreas and salivary glands of the rat and mouse. *Journal of toxicologic pathology* 2016; 29(1):1-124.
59. Sadek AS and Khattab RT. The protective role of melatonin on L-arginine-induced acute pancreatitis in adult male albino rats. *Folia Morphologica Journal* 2017; 76(1): 66-73.
60. Elbassuoni EA and Abdel Hafez SM. Impact of chronic exercise on counteracting chronic stress-induced functional and morphological pancreatic changes in male albino rats. *Cell Stress and Chaperones Journal* 2019; 24: 567-580.
61. Strobel O, Rosow DE, Rakhlin EY, Lauwers GY, Trainor AG, Alsina J, Castillo CF, Warshaw AL and Thayer SP. Pancreatic duct glands are distinct ductal compartments that react to chronic injury and mediate Shh-induced metaplasia. *Gastroenterology Journal* 2010; 138(3): 1166-1177.
62. Yin G, Hu G, Wan R, Yu G, Cang X, Ni J, Xiong J, Hu Y, Xing M, Fan Y, Xiao W, Qiu L, Wang S and Wang X. Role of bone marrow mesenchymal stem cells in L-arg-induced acute pancreatitis: Effects and possible mechanisms. *International Journal of Clinical and Experimental Pathology* 2015; 8(5): 4457-4468.
63. Tu XH, Song JX, Xue XJ, Guo XW, Ma YX, Chen ZY, Zou ZD and Wang L. Role of bone marrow-derived mesenchymal stem cells in a rat model of severe acute pancreatitis. *World Journal of Gastroenterology* 2012; 18(18): 2270-2279.
64. Qu B, Chu Y, Zhu F, Wang B, Liu T, Yu B and Jin S. Granulocyte colony-stimulating factor enhances the therapeutic efficacy of bone marrow mesenchymal stem cell transplantation in rats with experimental acute pancreatitis. *Oncotarget Journal* 2017; 28; 8(13): 21305-21314.
65. Qian D, Gong J, He Z, Hua J, Lin S, Xu C, Meng H and Zhenshun Song. Bone marrow-derived mesenchymal stem cells repair necrotic pancreatic tissue and promote angiogenesis by secreting cellular growth factors involved in the SDF-1 $\alpha$ /CXCR4 axis in rats. *Stem Cells International Journal* 2015; 2015: 306836.
66. Ahmed-Sorour HA and Abd-Elgalil MM. Mesenchymal stem cells ameliorate diabetic renocortical changes in a rat model: Histological, morphometrical and biochemical study. *Journal of Medical Histology* 2019; 3(2): 132-161.
67. Schneider G and Saur D. Mesenchymal stem cells: Therapeutic potential for acute pancreatitis. *Gastroenterology Journal* 2011; 140(3): 779-782.
68. Zhao H, He Z, Huang D, Gao J, Gong Y, Wu H, Xu A, Meng X and Li Z. Infusion of bone marrow mesenchymal stem cells attenuates experimental severe acute pancreatitis in rats. *Stem Cells International Journal* 2016a; 2016: 7174319.
69. Moustafa EM, Moawed FS and Abdel-Hamid GR. Icarin promote stem cells regeneration and repair acinar cells in l-arginine / radiation-inducing chronic pancreatitis in rats. *Dose Response Journal* 2020; 18(4): 1-13.
70. Ahmed SM, Morsi M, Ghoneim NI, Abdel-Daim MM and El-Badri N. Mesenchymal stromal cell therapy for pancreatitis: A systematic review. *Oxidative Medicine and Cellular Longevity Journal* 2018; 2018: 3250864.
71. Huh JW, Kim WY, Park YY, Lim CM, Koh Y, Kim MJ and Hong SB. Anti-inflammatory role of mesenchymal stem cells in an acute lung injury mouse model. *Acute and Critical Care Journal* 2018; 33(3): 154-161.
72. Haroun H, Mohamed E, El Shahat AE, Labib H and Atef M. Adverse effects of energy drink on rat pancreas and the therapeutic role of each of bone marrow mesenchymal stem cells and nigella sativa oil. *Folia Morphologica Journal* 2020; 79(2): 272-279.

## الملخص العربي

## دراسة هستولوجية وهستوكيميائية مناعية على التأثير العلاجي المحتمل للخلايا الجذعية الوسيطة المشتقة من نخاع العظم على التهاب البنكرياس الحاد المحدث بواسطة ل-أرجينين في ذكر الجرذ الأبيض البالغ

ليلى فتحي عمار، منى تيسير صادق، رضا حسن البقري، أماني محمد موسى

قسم الهستولوجيا وبيولوجيا الخلية- كلية الطب- جامعة طنطا

**المقدمة:** يعتبر التهاب البنكرياس الحاد حالة التهابية تهدد الحياة للغاية ولا يوجد علاج محدد لها. تمثل الخلايا الجذعية الوسيطة المشتقة من نخاع العظم علاجًا محتملاً لالتهاب البنكرياس الحاد لأنها تعزز إصلاح الأنسجة بسبب قدرتها على التجدد الذاتي وتعدد قدراتها.

**الهدف من العمل:** تم تنفيذ هذا العمل لدراسة التأثير العلاجي المحتمل للخلايا الجذعية الوسيطة المشتقة من نخاع العظم على التهاب البنكرياس الحاد المحدث بواسطة ل-أرجينين في ذكر الجرذ الأبيض البالغ.

**المواد والطرق:** تم استخدام خمسة وأربعين جرذاً من الذكور البيضاء البالغة وتم تقسيمهم إلى ثلاث مجموعات رئيسية. المجموعة الأولى لتمثل مجموعة التحكم وتضمنت ؛ المجموعة ١-أ (تم الاحتفاظ بالحيوانات بها كمصدر للخلايا الجذعية الوسيطة المشتقة من نخاع العظم) ، المجموعة الفرعية ١-ب (تلقت الحيوانات بها ٢,٥ مل من المحلول الملحي مرة واحدة داخل الغشاء البريتوني) والمجموعة الفرعية ١-ج (تلقت الحيوانات بها ٢,٥ مل من المحلول الملحي مرة واحدة داخل الغشاء البريتوني ثم بعد مرور ساعة تم حقن كل جرذ ب ١ مل من المادة الوسيطة المستخدمة لتعليق الخلايا الجذعية مرة واحدة في وريد الذيل. المجموعة الثانية: تم حقن الحيوانات ب ٢,٥ مل من ٢٠٪ ل-أرجينين مرة واحدة داخل الغشاء البريتوني بغرض احداث التهاب البنكرياس الحاد في حين المجموعة الثالثة: تم حقن الحيوانات ب ١ مل (١ × ١٠٦) من الخلايا الجذعية المعلقة في المادة الوسيطة في وريد الذيل بعد ساعة واحدة من احداث التهاب البنكرياس الحاد. تم أخذ عينات الدم من جميع المجموعات لقياس مستويات الأميليز والليباز في الدم عند ٢٤ ساعة و ٧٢ ساعة. تم التضحية بالجرذان عند ٧٢ ساعة وتم تحضير عينات البنكرياس للدراسة النسيجية والهستوكيميائية المناعية بواسطة المجهر الضوئي.

**النتائج:** أظهرت الجرذان التي عولجت بالخلايا الجذعية الوسيطة المشتقة من نخاع العظم تحسناً ملحوظاً في أنسجة البنكرياس وإنزيمات البنكرياس مقارنة بالمجموعة الثانية الغير المعالجة والتي أظهرت فقدان السمات الطبيعية للبنكرياس مع تغيرات نسيجية واضحة في العنبيات الإفرازية للبنكرياس.

**الخلاصة:** الخلايا الجذعية الوسيطة المشتقة من النخاع العظمي لها تأثيراً علاجياً محسناً جيداً علي العنبيات الإفرازية للبنكرياس بعد احداث التهاب البنكرياس الحاد.